RSC Advances

ROYAL SOCIETY OF CHEMISTRY

www.rsc.org/advances

Cite this: DOI: 10.1039/c0xx00000x

www.rsc.org/xxxxxx

ARTICLE TYPE

Photoluminescent graphene quantum dots for bioimaging applications

Shoujun Zhu,[a] Nan Zhou,[b] Zeyu Hao,[b] Suraj Maharjan,[b] Xiaohuan Zhao,[a] Yubin Song,[a] Bin Sun,[c] Kai Zhang,[a] Junhu Zhang,[a] Hongchen Sun,[c] Laijin Lu,*[b] Bai Yang*[a]

Received (in XXX, XXX) Xth XXXXXXXXX 20XX, Accepted Xth XXXXXXXXX 20XX

DOI: 10.1039/b000000x

Graphene quantum dots (GQDs), due to their ultrasmall size, excellent optical properties, chemical stability, biocompatibility, anti-photobleaching as well as low toxicity, have been widely used as a fluorescent bio-probe. In this study, we used the top-down "nano-cutting" route to prepare fluorescent GQDs. The as-prepared GQDs possessed ca. 4 nm diameter with 0.218 nm crystal lattice, and they owned outstanding solubility due to the plentiful oxygen and nitrogen based groups. The GQDs are exploited in bioimaging in vitro and in vivo. Using rat Schwann cells as the model system, the time-dependent cellular uptake of GQDs was tested by fluorescence activated cell sorter (FACS) and confocal laser scanning microscope (CLSM), and the it reached the saturation point after 24 h. Benefited by the excitation-dependent PL of the GQDs, the multi-color cell labeling was achieved, and the GQDs were proved to be mainly distributed in cytoplasm and lysosomes. Furthermore, using long wavelength emission (620 nm), the in vivo imaging was realized in nude mouse.

1. Introduction

A wide range of fluorescent carbon nanomaterials exhibit the fascinating optical properties, which are very promising for low toxicity fluorescent materials.[1, 2] The most common carbon nanomaterials are carbon dots (CDs),[3-5] which mainly contained graphene quantum dots (GQDs), carbon nanodots (CNDs), and polymer dots (PDs).[6] GQDs, labeled as rising fluorescent carbon materials, have drawn more and more attention these years.[7-11] The GQDs are also one of the heavy-metal-free fluorescent nanomaterials, which are one class of "zero-dimensional" CDs containing the integrated graphene core and connected surface groups.[12] GQDs were widely applied in the fields of bioimaging, biosensor, drug delivery as well as bio-diagnosis owing to their outstanding advantage such as the PL stability, low toxicity and good compatibility.[13] As a result, increasing reports have focused on the bio-based application of the GQDs.[9, 14-17] And the cellular uptake mechanism and internalization of GQDs begin to be investigated in detail.[18, 19] Furthermore, it is highly significant to apply the GQDs to bioimaging in vivo using the long wavelength light excitation, which can decrease the autofluorescence of the living body.[20]

In this work, the top-down "nano-cutting" route was used to prepare fluorescent GQDs.[14] The applied HNO_3/H_2SO_4 was a solution phase-based scissor, which exfoliated and cut the carbon resource, as well as modified the edge with oxygenic/nitrous groups, simultaneously.[21-23] The as-prepared GQDs owned outstanding solubility due to the plentiful oxygen and nitrogen based groups. The GQDs are exploited in bioimaging in vitro and in vivo. Benefited by the excitation-dependent PL of the GQDs, the multi-color cell labeling was achieved using rat Schwann cells as the model system, and the GQDs were proved to be mainly distributed in cytoplasm and lysosomes. Furthermore, using long wavelength emission, the in vivo imaging was realized in nude mouse.

2. Experimental detail

2.1. Preparation of GQDs. 300 mg graphite powder was dispersed in mixed acid (containing concentrated HNO_3 20 mL and concentrated H_2SO_4 60 mL). Then put the reaction system ultrasound for 30 min, followed by putting the solution into a 100 mL round-bottom flask, stirred at 120 °C for 12 h. After the reaction, dilute the solution by pouring it into 300 mL di-water, followed by neutralizing the acid with Na_2CO_3. Put the solution into the refrigerator to remove the Na_2SO_4 and $NaNO_3$ salt from the solution as much as possible (repeat three times). Aggregation in the solution was then excluded by filter membrane of 220 nm. Finally, 3500 dialysis bag was used to further purify the sample.

2.2. Characterization. High-resolution transmission electron microscope (HTEM) was recorded on JEOL JEM-2100F. Fluorescence spectroscopy was performed with a Shimadzu RF-5301 PC spectrophotometer. UV-vis absorption spectra were obtained using a Shimadzu 3100 UV-vis spectrophotometer. IR spectra were taken on a Nicolet AVATAR 360 FT-IR spectrophotometer. X-ray Photoelectron Spectroscopy (XPS) was investigated by using ESCALAB 250 spectrometer with a mono X-Ray source Al Kα excitation (1486.6 eV). Binding energy calibration was based on C1s at 284.6 eV.

2.3. Bio-based experimental section.

Materials: Fetal bovine serum (FBS), phosphate buffer solution (PBS), Dulbecco's Modified EagleMedium (DMEM), penicillin/streptomycin, trypsin/EDTA, anhydrous dimethyl

sulfoxide, Lysosome-Tracker were obtained from Life Technologies. 3-(4,5-dimethyl-2-thiazolyl)-2,5-diphenyl-2-H-tetrazolium bromide (MTT) and dimethyl sulfoxide (DMSO) were purchased from Sigma-Aldrich. Chloral hydrate was purchased from Sinopharm Chemical Reagent Co. (Shanghai, China).

Cytotoxicity: The RSC96 cell line was obtained from the Cell Bank of Chinese Academy of Science (Shanghai, China) and cultured in the DMEM supplemented with 10 % FBS, 100 U/mL penicillin, and 100 μg/mL streptomycin at 37 °C in a humidified atmosphere with 5% CO_2. Briefly, RSC96 cells were seeded in 96-wellplate at 1×10^4 cells/well in 200 μL culture medium under 37 °C and 5% CO_2. After 24 h incubation, different concentrations of GQDs (5, 10, 15, 20, 25, 35, 50, 70, 100, 150, 200, 300 μg/mL) was added and incubated for another 24 h at 37 °C. Then, GQDs dispersion in each well was replaced by 180 μL serum free medium (SFM) and 20 μL MTT (5 mg/mL). Cells were further incubated for 3 h; the supernatant was removed by inverting the plates to decant the liquid; 200 μL/well DMSO was added to dissolve the crystals remaining at the bottom of plate. The absorbance was measured at 490 nm using a Synergy HT microplate reader (Bio-Tek, Winooski, VT). Cell viability was expressed as a percentage relative to untreated cell, which served as the control.

Time-dependent Cellular Uptake: RSC96 cells (5×10^5 cells/well) were seeded in 6-well plates and incubated for 24 h. GQDs (20 μg/mL) was added and incubated for different time (0.5, 1, 6, 24, 48 h). Subsequently, the cells were washed 3 times with PBS, trypsinized, harvested, centrifuged, and resuspended in 200 μL of PBS. Finally, the MFI of 10000 cells at each time point was measured using a fluorescence activated cell sorter (FACS) Aria II flow cytometer with 488 nm laser and three channels (FITC, PE and Texas Red) were used to measure.

In Vitro Fluorescence Imaging: RSC96 cells (5×10^4 cells/dish) were seeded in a 35 mm glass-bottom dish and incubated for 24 h. GQDs (200 μg/mL) were added and incubated for 6 h. After that, the cells were rinsed 3 times with PBS and added 1 mL PBS for scanning. Live cell imaging was applied here to avoid the auto-fluorescence of the fixative paraformaldehyde and scanning was performed at different excitation/emission wavelengths, including 405/425-525 nm, 488/500-600 nm, 515/530-630 nm, 559/570-670 nm, and 635/650-750 nm, with a FV1000 Olympus IX81 CLSM (Osaka, Japan) using a 60× oil-immersion objective lens. Moreover, cells were double labeled with LysoTracker Red and GQDs to observe the accumulation of GQDs in lysosomes (The propidium iodide (PI), LysoTracker red were used to label nucleus and lysosomes, respectively).

In Vivo Fluorescence Imaging: Male BALB/c nude mice with the age of 5 weeks were purchased from Laboratory Animal Center of the Jilin University and were housed in the standard facility. Mice were subcutaneously injected with GQDs (1 mg/mL, 100 μL) on their back after being anesthetized by intraperitoneal injection of 4% chloral hydrate. The mice were imaged using IVIS Spectrum Imaging System (Perkin Elmer) with varied excitation light wavelengths from 465 nm to 500 nm and detected emission light wavelengths from 580 nm to 620 nm. The most suitable excitation/emission wavelength was 465/620 nm.

2.4. Live subjects.

The experiment was performed with approval from the Animal Care and Ethics Committee of Jilin University in China. All experiments were performed according to the National Institutes of Health Guide for the Care and Use of Laboratory Animals.

3. Result and discussion

The GQDs were prepared by a modified "nano-cutting" method from graphite powder and HNO_3/H_2SO_4, as shown in Fig. 1a. The average diameter of the prepared GQDs was ca. 3.93 nm with crystal lattice ca. 0.218 nm, which was attributed to (100) lattice plane of graphene (Fig. 1b-d).[24] In the FTIR analysis of GQDs, stretching vibrations of C-OH at 3406 cm^{-1}, C-H at 2914 cm^{-1} and 2858 cm^{-1}, as well as bending vibrations of N-H at 1570 cm^{-1} and a vibrational absorption band of C=O at 1624 cm^{-1} were all observed (Fig. S1).[25] In addition, surface groups were also investigated by XPS analysis (Fig. S2). The C1s analysis revealed three different types of carbon: graphitic or aliphatic carbon (C=C/C-C), oxygenated carbon and nitrous carbon; and the nitrous carbon contained pyridine-like, pyrrole and nitric nitrogen; the percentage of different groups were listed in the supporting information. All these oxygen and nitrogen based chemical groups endow the GQDs with outstanding solubility (over 20 mg/mL in aqueous solution), which will be very important for the practical applications.[26]

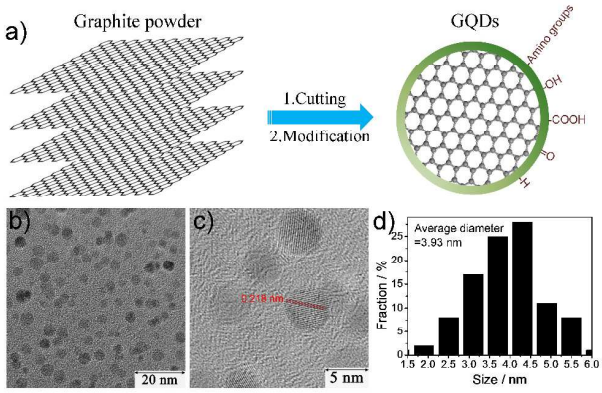

Fig. 1 a) The synthetic scheme for GQDs b-c) TEM images of GQDs at different amplification. d) The diameter distribution of GQDs determined by the TEM.

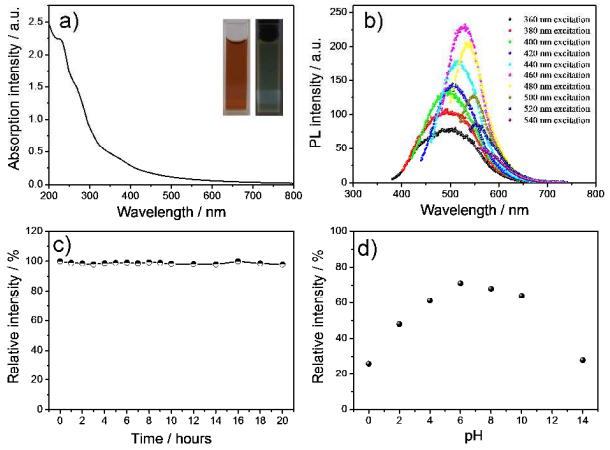

Fig. 2 The optical property of GQDs. a) UV/Vis absorption spectra of the GQDs; Insets show photographs of GQDs in

aqueous solutions under sunlight and UV light, respectively. b) The PL spectra of GQDs in aqueous solutions. c) The photo-stability of the GQDs under portable UV lamp. d) The pH-dependent PL behavior of the GQDs aqueous solution.

The optical properties of the GQDs were further investigated. In the UV-Vis spectra, there were obvious absorption peaks from UV to blue region in aqueous solution of GQDs (Fig. 2a), which contained the π-π*, n-π* as well as surface state transition.[27, 28] In the fluorescence spectra, GQDs possess the optimal emission wavelengths at ca. 530 nm (465 nm excitation), and showed green-yellow color under a hand-hold UV lamp (Fig. 2b and the inset of the Fig. 2a). The PL center of the GQDs was suggested to be the surface state,[29, 30] which was formed by the hybridization structure of edge groups and the connected graphene core, and the efficient edge groups for green emission were mainly carboxyl and amide.[31] Due to the wide size and surface chemical group distributions, the GQDs possessed excitation-dependent PL. Fortunately, the excitation-dependent PL behaviors can be applied in long wavelenght for biological imaging fields.

In addition, GQDs possessed high photo-stability (Fig. 2c), after 20 hours UV exposure (hand-hold UV lamp), the PL intensity and the peak shape were nearly unchanged. The intensities of green emission decrease in the solution of both high and low pH value (Fig. 3d), but kept stable in the range of 4-10. It indicated that the pH-dependent behaviors at specific ranges may contribute to the protonation/deprotonation of carboxyl groups, which affected the PL center of the green emission.[31-33]

The as-prepared GQDs possessed stable PL which has huge potetial for bio-based applications.[19, 34] The rat Schwann cells (RSC96) was chosen as model system to investigate the cellular toxicity and uptake of GQDs, and the results showed that the GQDs possessed low cell toxicity.[35] At the concentration of GQDs ranging from 10 to 100 μg/mL, the cell viability remained over 90 % (Fig. 3a). And the cell viability still kept over 60% with even 300 μg/mL adding. The low cytotoxicity is one of the most important characteristics of GQDs, which was consistent with the previous results.[9, 13] Furthermore, the time-dependent cellular uptake of GQDs was investigated, and the Fig. 3b showed the linear increase in the total intracellular amount of GQDs with incubation time in RSC96 cells. The uptake of GQDs reached the saturation point after 24 h. Time-dependent uptake of GQDs was also observed by confocal laser scanning microscope (CLSM). From Fig. 3c-h, partial green emission was observed in the cells after 1 h culturing with GQDs, and it reached the saturation point until 24 h culturing. Long time uptake (48 h) just kept the same emission intensity.

Due to the excitation dependent behaviors of the GQDs, they can be exploited to bio-label at different wavelength.[36] Fig. 4a-e shows the bioimaging results of the GQDs by CLSM at tunable excitation wavelengths. Subsequently, we investigated the intracellular distribution of GQDs by co-localizing with cell organelles specific dyes. The propidium iodide (PI), LysoTracker red were used to label nucleus and lysosomes, respectively (Fig. S3). As a result, the extensive co-localization of GQDs with the LysoTracker was observed, which suggested that endocytosed GQDs could partially transport to lysosomes (Fig. 4f).[37] The other GQDs were distributed in cytoplasm. However, it should be noted that the organic dyes can easily absorb on to GQD, so the co-localization might also be a false appearance. The energy depedent uptake behavior were also observed in the large polymer dots,[37, 38] which indicated that the size of the nanoparticles was very important for the cell uptake and internalization.

Furthermore, because the GQDs possess excitation-dependent PL, they can give deep-red emission, which is very important for decreasing the influence of body autofluorescence.[39-41] A nude mouse was subcutaneously injected with GQDs to investigate the in vivo imaging.[18] The mouse was anesthetized and imaged in vivo optical imaging system. Two excitations including blue and green light with center wavelengths at 465 and 500 nm, respectively, were applied during in vivo imaging (Fig. S4 and Fig. 5). The detected wavelength was tuned from 580 nm to 600 nm, and we found that the Ex/Em=465/620 nm showed the best bioimaging result with less autofuorescence background and increased signal-to-noise.[42]

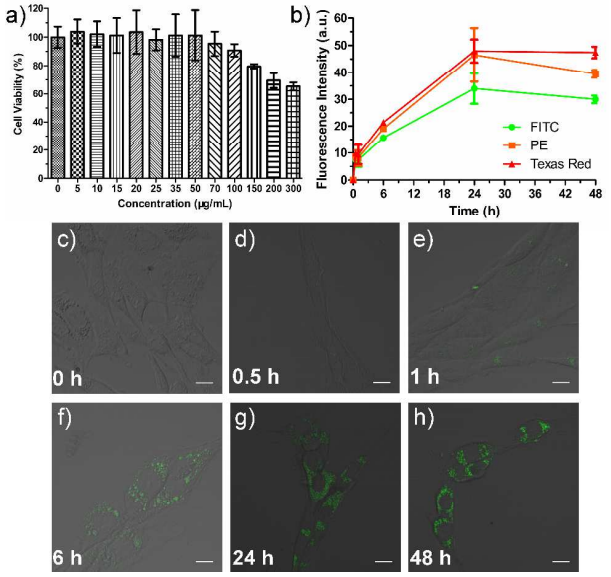

Fig. 3 a) The cell cytotoxicity of GQDs determinted by MTT. b) The time-dependent cellular uptake of GQDs by fluorescence activated cell sorter (FACS). The values are expressed as mean ± SD (n = 3). c-h) Time-dependent uptake of GQDs was observed

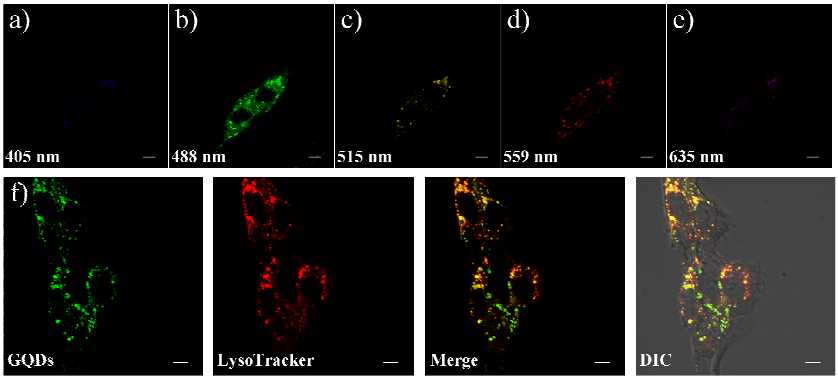

by CLSM. The scale bar is 10 μm.

Fig. 4 The bioimaging of GQDs in vitro in RSC96 cells. a-e) The multi-color bioimaging of GQDs (by different excitation wavelength, 405, 488, 515, 559 and 635 nm, respectively) determined by CLSM (The scale bar is 5 μm). f) GQDs co-localized with cellular organelles specific dyes: LysoTracker was used to label the lysosomes, and the GQDs were mainly distributed in lysosomes. The scale bar is 5 μm.

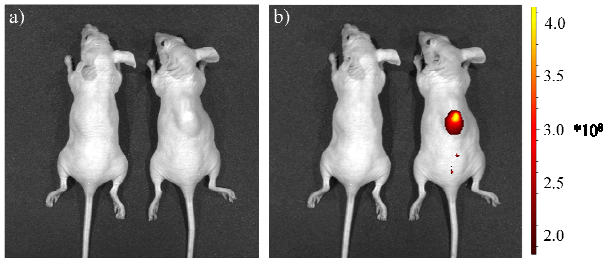

Fig. 5 a-b) In vivo imaging of GQDs in BALB/c mice. Left mouse is saline-injected and right mouse is GQDs-injected, a) is bright field and b) is visible light excitation (Ex/Em=465/620 nm).

4. Conclusions

In conclusion, a top-down route to GQDs was developed based on the acid-assisted cutting methods. The as-prepared GQDs possessed ca. 4 nm diameter with 0.218 nm crystal lattice, and they owned outstanding solubility due to the plentiful oxygen and nitrogen based groups. The GQDs are exploited in bioimaging in vitro and in vivo. Benefited by the excitation-dependent PL of the GQDs, the multi-color cell labeling was achieved using rat Schwann cells as the model system, and the GQDs were proved to be mainly distributed in cytoplasm and lysosomes. Furthermore, using long wavelength emission, the in vivo imaging was realized in nude mouse. In the future work, we will focus on the GQDs with target, bio-label and diagnosis multi-functional properties.

Acknowledgements

The authors thank Yu Fu from our lab for the useful comments for this work. This work was supported by the National Science Foundation of China (Grand No. 51373065, 21221063, 81171145, 81371363), the National Basic Research Program of China (973 Program, Grant No. 2012CB933800), and the Specialized Research Fund for the Doctoral Program of Higher Education (no. 20130061130010).

Notes and references

[a] *State Key Laboratory of Supramolecular Structure and Materials, College of Chemistry, Jilin University, 2699 Qianjin Street, Changchun 130012, China*
Email: byangchem@jlu.edu.cn
[b] *Department of Hand Surgery, the First Hospital of Jilin University*
Email: lulaijin@hotmail.com
Changchun, 130021, P.R. China
[c] *School of Stomatology, Jilin University, Changchun, 130041, P. R. China*

† Electronic Supplementary Information (ESI) available: FT-IR spectra and XPS analysis of GQDs, as well as in vivo imaging of GQDs in BALB/C mice at different excitatoin and emission wavelength. See DOI: 10.1039/b000000x/

‡ S. Zhu and Nan Zhou contributed equally to this work.

1. K. Welsher, Z. Liu, S. P. Sherlock, J. T. Robinson, Z. Chen, D. Daranciang and H. Dai, *Nature Nanotech.*, 2009, **4**, 773-780.
2. T. Gokus, R. R. Nair, A. Bonetti, M. Bohmler, A. Lombardo, K. S. Novoselov, A. K. Geim, A. C. Ferrari and A. Hartschuh, *ACS Nano*, 2009, **3**, 3963-3968.
3. S. N. Baker and G. A. Baker, *Angew. Chem. Int. Ed.* , 2010, **49**, 6726-6744.
4. H. Li, Z. Kang, Y. Liu and S.-T. Lee, *J. Mater. Chem.*, 2012, **22**, 24230-24253.
5. L. Cao, M. J. Meziani, S. Sahu and Y. P. Sun, *Acc. Chem. Res.*, 2013, **46**, 171-180.
6. S. Zhu, Y. Song, X. Zhao, J. Shao, J. Zhang and B. Yang, *Nano Res.*, 2015, **8**, 355-381.
7. D. Pan, J. Zhang, Z. Li and M. Wu, *Adv. Mater.*, 2010, **22**, 734-738.
8. Y. Li, Y. Hu, Y. Zhao, G. Shi, L. Deng, Y. Hou and L. Qu, *Adv. Mater.*, 2011, **23**, 776-780.
9. S. Zhu, J. Zhang, C. Qiao, S. Tang, Y. Li, W. Yuan, B. Li, L. Tian, F. Liu, R. Hu, H. Gao, H. Wei, H. Zhang, H. Sun and B. Yang, *Chem. Commun.*, 2011, **47**, 6858-6860.
10. S. Zhu, S. Tang, J. Zhang and B. Yang, *Chem. Commun.*, 2012, **48**, 4527-4539.
11. S. Zhu, J. Zhang, X. Liu, B. Li, X. Wang, S. Tang, Q. Meng, Y. Li, C. Shi, R. Hu and B. Yang, *RSC Adv.*, 2012, **2**, 2717.
12. Z. Zhang, J. Zhang, N. Chen and L. Qu, *Energy Environ. Sci.*, 2012, **5**, 8869-8890.
13. L. Lin, M. Rong, F. Luo, D. Chen, Y. Wang and X. Chen, *TrAC Trends in Analytical Chemistry*, 2014, **54**, 83-102.
14. J. Peng, W. Gao, B. K. Gupta, Z. Liu, R. Romero-Aburto, L. Ge, L. Song, L. B. Alemany, X. Zhan, G. Gao, S. A. Vithayathil, B. A. Kaipparettu, A. A. Marti, T. Hayashi, J. J. Zhu and P. M. Ajayan, *Nano Lett.*, 2012, **12**, 844-849.
15. M. Zhang, L. Bai, W. Shang, W. Xie, H. Ma, Y. Fu, D. Fang, H. Sun, L. Fan, M. Han, C. Liu and S. Yang, *J. Mater. Chem.*, 2012, **22**, 7461.
16. X. Chen, X. Zhou, T. Han, J. Wu, J. Zhang and S. Guo, *ACS Nano*, 2013, **7**, 531-537.
17. Z. M. Markovic, B. Z. Ristic, K. M. Arsikin, D. G. Klisic, L. M. Harhaji-Trajkovic, B. M. Todorovic-Markovic, D. P. Kepic, T. K. Kravic-Stevovic, S. P. Jovanovic, M. M. Milenkovic, D. D. Milivojevic, V. Z. Bumbasirevic, M. D. Dramicanin and V. S. Trajkovic, *Biomaterials*, 2012, **33**, 7084-7092.
18. M. Nurunnabi, Z. Khatun, K. M. Huh, S. Y. Park, D. Y. Lee, K. J. Cho and Y. K. Lee, *ACS Nano*, 2013, **7**, 6858-6867.
19. C. Wu, C. Wang, T. Han, X. Zhou, S. Guo and J. Zhang, *Adv. Healthcare Mater.*, 2013, **2**, 1613-1619.
20. C. Ding, A. Zhu and Y. Tian, *Acc. Chem. Res.*, 2014, **47**, 20-30.
21. R. Ye, C. Xiang, J. Lin, Z. Peng, K. Huang, Z. Yan, N. P. Cook, E. L. Samuel, C. C. Hwang, G. Ruan, G. Ceriotti, A. R. Raji, A. A. Marti and J. M. Tour, *Nature Commun.*, 2013, **4**, 2943.
22. D. B. Shinde and V. K. Pillai, *Chem. Eur. J.*, 2012, **18**, 12522-12528.
23. T. S. Sreeprasad, A. A. Rodriguez, J. Colston, A. Graham, E. Shishkin, V. Pallem and V. Berry, *Nano Lett.*, 2013, **13**, 1757-1763.
24. L. Lin and S. Zhang, *Chem. Commun.*, 2012, **48**, 10177-10179.
25. L. Fan, Y. Hu, X. Wang, L. Zhang, F. Li, D. Han, Z. Li, Q. Zhang, Z. Wang and L. Niu, *Talanta*, 2012, **101**, 192-197.
26. L.-L. Li, J. Ji, R. Fei, C.-Z. Wang, Q. Lu, J.-R. Zhang, L.-P. Jiang and J.-J. Zhu, *Adv. Funct. Mater.*, 2012, **22**, 2971-2979.
27. Y. Wang, S. Kalytchuk, Y. Zhang, H. Shi, S. V. Kershaw and A. L. Rogach, *J. Phys. Chem. Lett.*, 2014, **5**, 1412-1420.
28. P. Luo, Y. Qiu, X. Guan and L. Jiang, *PCCP*, 2014, **16**, 19011-19016.
29. Z. Qian, J. Ma, X. Shan, L. Shao, J. Zhou, J. Chen and H. Feng, *RSC Adv.*, 2013, **3**, 14571.
30. J. Gu, M. J. Hu, Q. Q. Guo, Z. F. Ding, X. L. Sun and J. Yang, *RSC Adv.*, 2014, **4**, 50141-50144.
31. L. Wang, S. J. Zhu, H. Y. Wang, S. N. Qu, Y. L. Zhang, J. H. Zhang, Q. D. Chen, H. L. Xu, W. Han, B. Yang and H. B. Sun, *ACS Nano*, 2014, **8**, 2541-2547.

32. L. Wang, S.-J. Zhu, H.-Y. Wang, Y.-F. Wang, Y.-W. Hao, J.-H. Zhang, Q.-D. Chen, Y.-L. Zhang, W. Han, B. Yang and H.-B. Sun, *Adv. Opt.Mater.*, 2013, **1**, 264-271.
33. S. Zhu, J. Zhang, S. Tang, C. Qiao, L. Wang, H. Wang, X. Liu, B. Li, Y. Li, W. Yu, X. Wang, H. Sun and B. Yang, *Adv. Funct. Mater.*, 2012, **22**, 4732-4740.
34. H. Sun, L. Wu, N. Gao, J. Ren and X. Qu, *ACS Appl. Mater. Inter.*, 2013, **5**, 1174-1179.
35. V. Kumar, V. Singh, S. Umrao, V. Parashar, S. Abraham, A. K. Singh, G. Nath, P. S. Saxena and A. Srivastava, *RSC Adv.*, 2014, **4**, 21101.
36. Y. Sun, S. Wang, C. Li, P. Luo, L. Tao, Y. Wei and G. Shi, *PCCP*, 2013, **15**, 9907-9913.
37. S. Zhu, L. Wang, N. Zhou, X. Zhao, Y. Song, S. Maharjan, J. Zhang, L. Lu, H. Wang and B. Yang, *Chem. Commun.*, 2014, **50**, 13845-13848.
38. S. Zhu, J. Zhang, L. Wang, Y. Song, G. Zhang, H. Wang and B. Yang, *Chem. Commun.*, 2012, **48**, 10889-10891.
39. M. Zheng, S. Liu, J. Li, D. Qu, H. Zhao, X. Guan, X. Hu, Z. Xie, X. Jing and Z. Sun, *Adv. Mater.*, 2014, **26**, 3554-3560.
40. B. Kong, A. Zhu, C. Ding, X. Zhao, B. Li and Y. Tian, *Adv. Mater.*, 2012, **24**, 5844-5848.
41. J. Tang, B. Kong, H. Wu, M. Xu, Y. Wang, Y. Wang, D. Zhao and G. Zheng, *Adv. Mater.*, 2013, **25**, 6569-6574.
42. T. Shao, G. Wang, X. An, S. Zhuo, Y. Xia and C. Zhu, *RSC Adv.*, 2014, **4**, 47977-47981.

The GQDs are exploited in bioimaging in vitro and in vivo: using the excitation-dependent PL, the multi-color cell labeling was achieved; using long wavelength emission, the in vivo imaging was realized.